Renewable Energy 230 (2024) 120784

Contents lists available at ScienceDirect

Renewable Energy

journal homepage: www.elsevier.com/locate/renene

Grid impact of co-located offshore renewable energy sources

Erik Jonasson *, Christoffer Fjellstedt, Irina Temiz

Department of Electrical Engineering, Uppsala University, Ångströmslaboratoriet, Lägerhyddsvägen 1, Uppsala, 75237, Sweden

ARTICLE INFO

Keywords:
Hybrid power plant
Offshore wind
Offshore floating photovoltaic
Wave energy
Capacity credit

ABSTRACT

As the share of renewable energy sources in the energy mix increases, weather-dependent variations in several time scales will have a significant impact on the power system. One way of mitigating these variations is to co-locate complementary energy sources at the same location. In this study, the complementarity between offshore floating photovoltaics, wave, and wind power is analyzed and the grid impact of such co-located energy sources is addressed using capacity credit. Additionally, the possibility of installing supplementary generation capacity within existing offshore wind power farms is investigated. It is found that co-locating wave power with offshore wind results in increased capacity credit compared to stand-alone wind power farms and that in all analyzed cases, the capacity credit of the co-located energy sources exceeds the capacity credit contribution of the separate energy sources. Co-locating photovoltaics with offshore wind brings little benefit to the capacity credit, but shows potential in increasing the utilization of the transmission cable.

1. Introduction

In the face of escalating climate change concerns and the urgent need for sustainable energy solutions, integrating renewable energy sources (RESs) into the electrical grid has become paramount in shaping the future of global energy landscapes [1]. Due to limited land availability in many parts of the world, the attention to deploying RESs offshore has increased. The dominating energy source in the offshore segment today is offshore wind, which is projected to continue increasing in deployments and be a vital part of the energy transition [1]. The European Union has set ambitious targets of achieving 60 GW of installed capacity of offshore wind by 2030, and 300 GW by 2050, in the member countries [2]. As increased levels of variable renewable energy sources (VRESs), such as offshore wind, are integrated into the power grid, these VRESs can be expected to have a significant effect on several aspects of the power system. An emerging trend both in academia and industry to mitigate some of the negative effects is to study co-located energy sources forming a hybrid power plant (HPP) [3].

The most commonly studied type of HPP is the combination of land-based wind power and photovoltaic (PV) [4]. The authors of [5] found that combining wind, PV, and gravitational energy storage in mountainous regions is an economically viable option. The use of battery energy storage systems (BESSs) has also been shown to effectively reduce the intermittency of wind-solar HPPs in Australia and increase profitability [6]. In studies analyzing co-located offshore energy sources, however, the majority investigate the combination of wave and offshore wind, see, for example, [7,8]. Other studies have also assessed the feasibility of adding OFPV to existing wind power farms [9], and analyzed how the complementarity of wind power, OFPV and in-stream tidal can be used [10].

The complementary nature of wave power and offshore wind have been studied from various aspects. Astariz and Iglesias studied the reduced mechanical loading of wind turbines (WTs) sheltered by WECs, known as the shadow effect [11]. The same effect has been experimentally investigated where it was shown that the forces acting on the turbine are reduced by up to 40% [12]. Another dimension of the complementary nature is the possibility of smoothening the power profile of the HPP compared to the energy sources comprising the HPP. Stoutenburg et al. [13] studied the reduction in power output variability resulting from co-locating wind and wave power in California and found that the reduction in variability is equivalent to geographically dispersing two wind power farms approximately 500 km or wave power farms 800 km. Another study introduced a power fluctuation factor to quantify the variability and found that an HPP consisting of 90% wave and 10% wind minimized the variability, with the drawback of lower annual electricity generation [14].

The effects and benefits derived from co-locating wave and wind power are, however, highly dependent on local weather patterns and metocean conditions. In [15], the combined wind and wave energy resources along the Latin American and European coasts were evaluated, and the European sites indicated better performance during winter months, whereas the Latin American sites showed greater year-round

* Corresponding author.
E-mail addresses: erik.jonasson@angstrom.uu.se (E. Jonasson), Christoffer.fjellstedt@angstrom.uu.se (C. Fjellstedt), Irina.temiz@uu.se (I. Temiz).

https://doi.org/10.1016/j.renene.2024.120784
Received 9 February 2024; Received in revised form 8 May 2024; Accepted 6 June 2024
Available online 8 June 2024

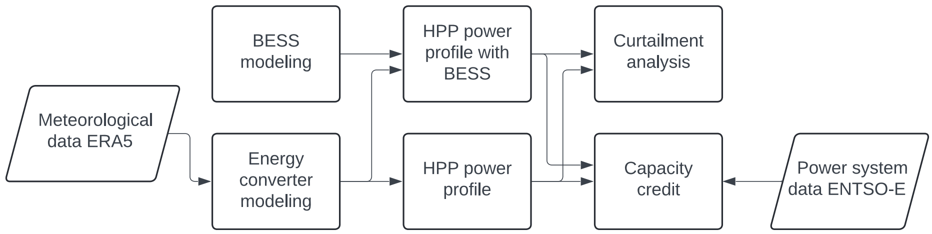

Fig. 1. Overall framework of the applied method.

potential. Along the southeast coast of China, the synergy of wave and wind energy availability has been shown to potentially reduce the variability and increase annual energy production, even though optimal locations for wind energy deployments differ from the optimal locations for wave energy deployments [16].

Although not investigated as extensively as wave-wind, the complementary nature of offshore wind power and OFPV has been analyzed to a certain extent. The reduction of variability has been quantified to be up to 63%, as well as increasing the energy generation per unit area by seven to ten times compared to a wind power farm [17]. Golroodbari et al. [9] found that adding OFPV to an existing wind power farm in the North Sea can be beneficial both in technical and economic terms by increasing the utilization of the grid connection point.

Even though the various benefits of HPPs have been investigated in the literature, few studies have been performed to measure the grid impact. In a case study of combining wind and wave energy in Ireland, the benefits of reduced variability, and as a consequence, increased capacity credit were discussed [18]. In [19], it was shown that combining VRESs reduces the operating reserves requirements, which also may increase the capacity credit. Despite previous efforts, a research gap exists regarding the impact of co-locating variable renewable energy sources on capacity credit.

1.1. Scope of the study

In the present study, the grid impact of three different HPPs is analyzed. The analysis focuses on time scales of hourly to intra-annual variations. The impact of VRESs on the grid in this time scale is primarily related to energy management issues such as energy availability and penetration levels. The energy generation is modeled on an hourly basis and the complementarity between the different energy sources is analyzed using conditional relative frequency distributions. The geographic area under consideration is the Netherlands and additional renewable energy is restricted to be deployed in the Dutch EEZ. Compared to other European countries, the Netherlands has a high share of fossil fuel in their generation mix and a scarcity of available land surface [20]. Moreover, the wind energy resources in the North Sea have been classified as good [21]. Therefore, the Netherlands could potentially benefit from co-located renewable energy generation offshore. This study aims to analyze the complementary nature between OFPV, wind, and wave power. The grid impact of co-locating these VRESs is addressed using capacity credit and increased utilization of a fixed capacity grid connection point. Additionally, the added benefit of including a BESS in a HPP is investigated.

2. Method and theory

The overall framework of the applied method is shown in Fig. 1. Detailed descriptions of each step are provided in this section.

2.1. Grid impact

In general, integration studies of renewable energy in the electrical grid can be analyzed from two perspectives: in terms of the aspect of space and time [22]. In space, the central question is how the generated power is delivered to the load. A characteristic of RESs is that resource-rich areas are often located far from population-rich areas [22]. The spatial distribution of RESs thus poses challenges for the integration of renewable energy. The time scale perspective is highly associated with the intermittent characteristic of VRESs. The effects of the intermittency on the grid and how the issues are addressed are dependent on the properties of the specific energy resource and the time scale that is considered. At one extreme of the time spectrum, this encompasses activities such as planning and building new generation units and transmission and distribution grids, and the time scale for these types of activities is decades [22]. On the other side of the time spectrum, power quality issues such as frequency stability and harmonics are pertinent [23]. An overview of issues associated with specific timescales, and the ones considered in this study, is shown in Fig. 2.

2.2. Capacity credit

The capacity credit definition in this study is derived from effective load carrying capability (ELCC). The ELCC of a generating unit is equivalent to the increase in constant load that the system can carry without a decrease in reliability [25], commonly measured in loss of load probability (LOLP). In order to accurately determine the capacity credit of a new generating unit, extensive information on electrical load and a complete inventory of existing generating units and their reliability is needed [26]. A simplified framework is employed in this study as follows:

- The load profile and energy generation per type are accessed as hourly time series.
- The dispatchable generation capacity is defined as being able to supply the highest net load (load minus production from non-dispatchable generation units).
- The added constant load, c, that can be added to the system after the addition of further renewable generation g_{added}, without decreasing the system reliability, is found iteratively according to the following equation

$$LOLP(\bar{L} + c, \bar{g} + g_{added}) = LOLP(\bar{L}, \bar{g}), \tag{1}$$

  where $\bar{L}$ is the time series of the load of the power system, $\bar{g}$ is the generation of VRESs existing in the power system and the derived dispatchable capacity. The ELCC of the added generation unit with modeled time-series generation g_{added} and rated capacity P_g is then the added constant load c.
- The capacity credit, cc, of said generation unit is calculated as $cc = c/P_g$.

Other definitions of capacity credit exist, which, for example, are derived from annual peak risk-based approaches, equivalent firm capacity, and secured capacity [27]. However, the approach using ELCC provides a more understandable and realistic estimation of the capacity credit than, for example, secured capacity [28].

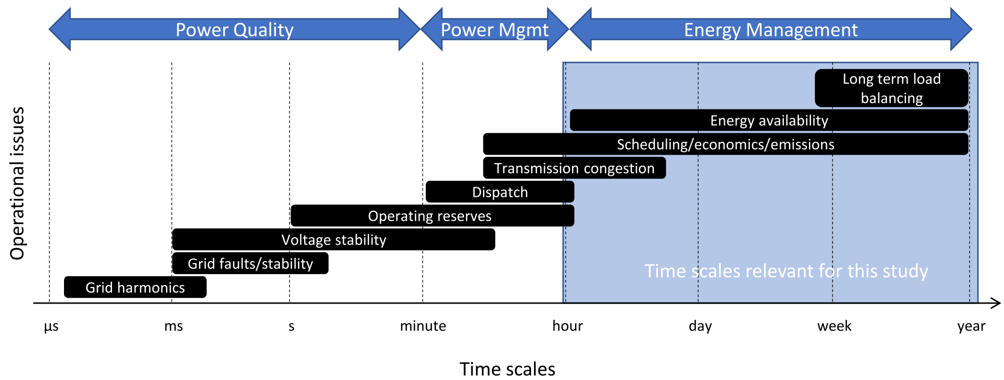

Fig. 2. Operational issues for the electrical grid on different time scales.
Source: Reworked with inspiration from [23,24].

2.3. Data

The data used in this study consist of meteorological reanalysis data from the reanalysis dataset ERA5 [29] and electrical generation and load of the Netherlands from the ENTSO-E transparency platform [30].

Even though ENTSO-E is perhaps the most ambitious power system data platform, there are shortcomings in data quality and availability [31]. The data used in this study are *Actual Total Load* and *Actual Generation per Production Type* for the bidding zone NL covering the years 2017–2021. For *Actual Total Load* the data availability was 100%. A few instances in the data *Actual Generation per Production Type* were missing (less than 0.01% of all instances). The missing data is replaced with the previous value.

In order to model large-scale renewable energy generation, meteorological reanalysis data is downloaded from ERA5, corresponding to the area of the Dutch EEZ. The time period of the reanalysis data matches that of the generation and the electrical load used in the study, namely 2017–2021. Parameters 100 m u- and v-component of wind are used to determine the wind speeds at 100 m above sea level, significant wave height and wave energy period are used to determine the mean wave power availability, and downwards solar radiation, as well as ambient air temperature, is used to estimate the OFPV mean power output.

2.4. Energy converter modeling

2.4.1. Wave power

Wave power modeling is performed using a power matrix that relates the peak wave period, T_p, and significant wave height, H_s, to the output power, shown in Fig. 3. The WEC design that is used in this study is the point-absorber type developed by CorPower Ocean [32]. In normal operation, the device is actively tuned to oscillate in resonance with the waves. During storm conditions, the device is detuned to create transparency to incoming waves to increase its survivability [32]. A single device is rated for 400 kW, but several devices are envisioned to be interconnected to form a wave power farm. The power output of several WECs in a farm is directly scaled with the number of units, as wake effects and other farm interactions can be made small by maintaining the number of rows small, and the spacing between devices sufficiently large [33].

2.4.2. Photovoltaics

The power output from OFPV is mainly dependent on the solar irradiation and the cell temperature. The technology is similar to regular land-based PV but is placed on moored floating pontoons [35]. The panels are in this study considered horizontally aligned parallel to the sea surface. The hourly mean power output has been calculated as

$$P_{PV} = \eta \cdot A \cdot G, \tag{2}$$

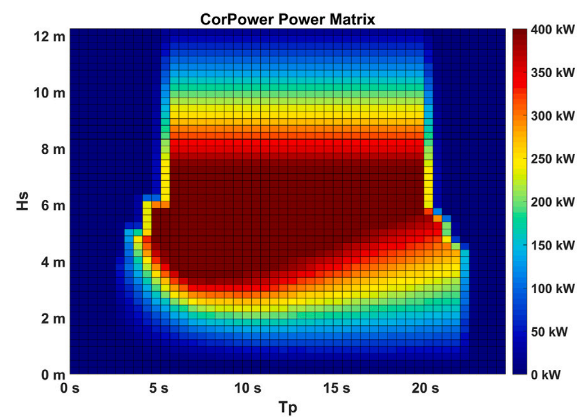

Fig. 3. Power matrix of the CorPower WEC. From Ref. [34], used under Creative Commons CC-BY license.

where A is the panel area, G is the global horizontal irradiance, and η is the PV temperature dependent efficiency. The efficiency η can be calculated as

$$\eta = \eta_{STC} \left(1 - \beta \left(T_a - T_{STC} + (T_N - T_a) \frac{I_T}{I_{T,N}} \right) \right), \tag{3}$$

where β is the temperature coefficient, I is irradiance, and T is temperature. Subscripts STC, N, and a, denote standard testing, nominal, and ambient operating conditions, respectively. For further details, the reader is referred to [36]. This study uses specifications from the PV panel JAM72S30-535, with an efficiency of 20.7% at standard testing conditions and a panel area of 2.6 m^2.

2.4.3. Wind power

The mean hourly power output from a WT is modeled using wind speed at hub height and the power curve for an 8 MW fixed platform offshore referential turbine from NREL [37]. The wind speeds at hub height is calculated using the following equation:

$$V_{hh} = V_{ref} \left(\frac{Z_{hh}}{Z_{ref}} \right)^{\alpha}, \tag{4}$$

where Z_{hh} is the hub height, and Z_{ref} is the reference height. V_{hh} and V_{ref} are the wind speed at hub height and reference level, respectively, and α is the power law exponent. It has previously been concluded that for offshore conditions a suitable value for α is 0.11 [38].

To account for wind speed variations within a wind farm, a multi-turbine power curve can be used [39]. As proposed in [40], if not all parameters are known it may be further simplified by introducing a standard deviation in the incoming wind speeds, σ_u. The power curve can be re-calculated using a normal distribution of the wind speeds. As

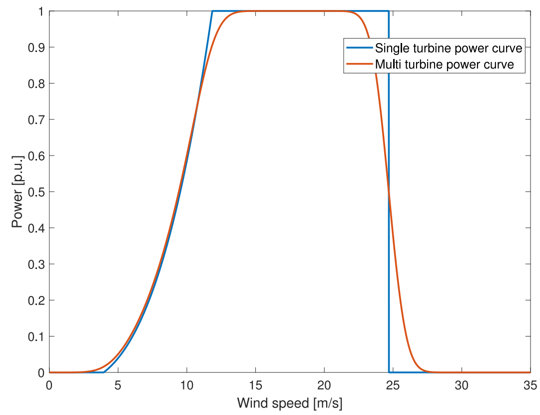

Fig. 4. Power curve of a single turbine and the resulting multi-turbine power curve.

in [41], the standard deviation of incoming wind speeds is in this study assumed to be 1 m/s. A multi-turbine power curve is constructed using the following equation:

$$P_{mt}(v) = \int_{v-5}^{v+5} f(x|v,\sigma_u^2)P_{st}(x)dx, \tag{5}$$

where P_{mt} and P_{st} represent the power at wind speed v for a multi-turbine and single-turbine power curve, respectively. The normalized power output from a single turbine power curve and the resulting multi-turbine power curve are shown in Fig. 4.

2.4.4. BESS

In addition to the energy converters, the inclusion of a BESS is implemented. The size of the BESS is fixed at 50 MWh, 150 MWh, and, 300 MWh. The maximum charge and discharge rate is 0.25C, meaning the BESS can fully discharge or recharge in four hours. The implementation is a simple state of charge (SoC) model, without consideration of round trip efficiency and self-discharge. The SoC is restricted to 0.2–1, and the discharge and charge cycle is determined in each time step according to one of two separate energy management strategies (EMSs). The first EMS aims to increase the capacity credit. This is achieved by maintaining the battery at full SoC, and discharge only when the system load exceeds the available power. The EMS is implemented as

$$P_{batt}(t) = \begin{cases} P_d & \text{if } P_{load}(t) > P_{gen}(t) \\ P_c & \text{if } P_{load}(t) < P_{gen}(t), \\ & \& \ SoC < 1 \\ 0 & \text{otherwise} \end{cases}, \tag{6}$$

where P_{batt} is the desired power output from the BESS, P_{load} is the power system load, and P_{gen} the total available generation capability of the power system. P_d is the appropriate discharge power that supports the system with the power deficit, given that the SoC is sufficiently high. If the power deficit is larger than what the BESS can provide, P_d is determined by the C-rate. P_c is the appropriate charging power, which is sufficiently small to not introduce further peak loads or overcharge the BESS.

The second EMS is intended to reduce curtailment losses for a given grid connection capacity. The EMS maintains the battery at minimum SoC and charges only when the power generation of the HPP exceeds the grid connection capacity. It is implemented as

$$P_{batt}(t) = \begin{cases} P_d & \text{if } P_{HPP}(t) < P_{GCC}, \\ & \& \ SoC > 0.2 \\ P_c & \text{if } P_{HPP}(t) > P_{GCC} \\ 0 & \text{otherwise} \end{cases}, \tag{7}$$

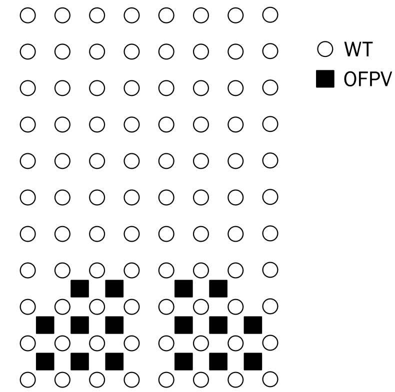

Fig. 5. Conceptual layout of case 1B.

where P_{HPP} is the power output of the HPP and P_{GCC} is the grid connection capacity of the park. P_c is determined such that the total power is as close to P_{GCC} as possible, while not overcharging the BESS. P_d is the maximum discharge power, given that the grid connection capacity, or BESS C-rate, is not exceeded.

For both strategies, the SoC in the subsequent time step as calculated as

$$SoC(t+1) = \frac{SoC(t) \cdot E_{batt} - P_{batt}(t) \cdot \Delta t}{E_{batt}}, \tag{8}$$

where E_{batt} is the rated energy of the battery and Δt the time duration of one step. The sign convention used is that charging power is negative, and discharging is positive.

2.5. Studied cases

The grid impact of co-located offshore VRESs is studied using three different cases of co-located VRESs numbered 1–3. Each case has three subcases, denoted A–C, corresponding to wind power installed capacity of 500 MW, 700 MW, and 1000 MW, respectively. As the dominating offshore energy source as of today is wind power [1], wind power farms with the installed capacity of 500 MW, 700 MW, and 1000 MW, act as benchmarks in this study for comparison with the cases with co-located VRESs.

Since there are yet no examples of co-located OFPV, wave, and wind power the formation of the studied cases is based on what industry partners and researchers in the EU-SCORES project envision to be feasible in the near future for new construction or for adding co-located energy production to an existing wind power farm [42].

2.5.1. Case 1 – Wind and OFPV

The first case consists of 700 MW OFPV co-located with wind power. Previous research has shown that similar proportions of installed capacity of wind power and PV are promising in terms of reduced variability [43]. Considering the spacing of the WTs in the plant of 6–7 times the rotor diameter [43] and an exclusion zone of 300 m surrounding the turbine, it is possible to fit approximately 45 MW OFPV in between four turbines. A conceptual layout of an HPP consisting of 700 MW wind and OFPV is illustrated in Fig. 5. Shading of OFPV panels due to WTs has not been accounted for.

2.5.2. Case 2 – Wind and wave

The second case consists of 70 MW wave power co-located with wind power. Approximately 175 WECs of the CorPower type would need to be used. Considering the same WT spacing as in case 1, and a WEC spacing of 15 times the width of the WEC, wake effects would be negligible [33]. A conceptual layout of such a plant is shown in Fig. 6, where each WEC cluster represents five WECs. The actual layout

Table 1
Summary of the considered plant configurations.

Case	Case 1			Case 2			Case 3			Benchmark		
Subcase	A	B	C	A	B	C	A	B	C	A	B	C
Wind power [MW]	500	700	1000	500	700	1000	500	700	1000	500	700	1000
Wave power [MW]	–	–	–	70	70	70	70	70	70	–	–	–
OFPV [MW]	700	700	700	–	–	–	700	700	700	–	–	–
Installed capacity [MW]	1200	1400	1700	570	770	1070	1270	1470	1770	500	700	1000

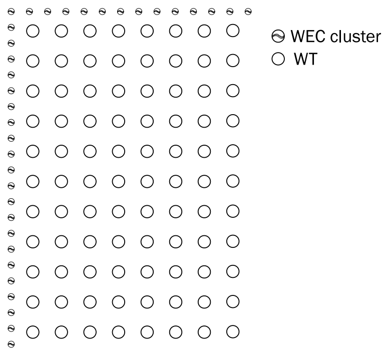

Fig. 6. Conceptual layout of case 2B.

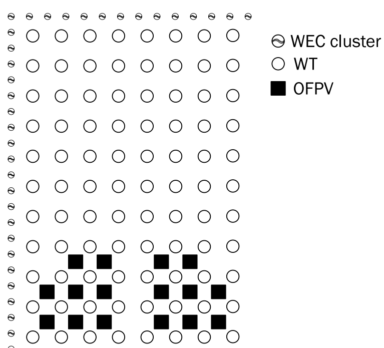

Fig. 7. Conceptual layout of case 3B.

of such an HPP would be dependent on factors such as distance to shore and local conditions. The WECs are assumed to be placed between the most frequent direction of incoming waves and the WTs, why wave attenuation due to WTs interaction can be neglected.

2.5.3. Case 3 – Wind, OFPV and wave

The third case is a combination of case 1 and case 2, with 700 MW OFPV and 70 MW wave power co-located with wind power. An illustration of the plant layout can be seen in Fig. 7.

In Table 1, all cases and the benchmark wind power farms are summarized. The illustrations in Figs. 5–7 are included solely to illustrate the scale of each energy type in the HPPs.

3. Results

3.1. Wave, wind and solar energy climate

Averaged over the geographical area of the Dutch EEZ, the mean wind speed at 100 m elevation is 8.3 m/s, which corresponds well to what is reported in the Dutch Offshore Wind Atlas [44]. The average global horizontal irradiation is 3.2 kWh/m^2/day. The wave climate with occurrences of wave heights and wave periods, together with the energy flux per meter of wave crest assuming deep water conditions, is shown in Fig. 8. The mean wave energy flux is 8.8 kW/m.

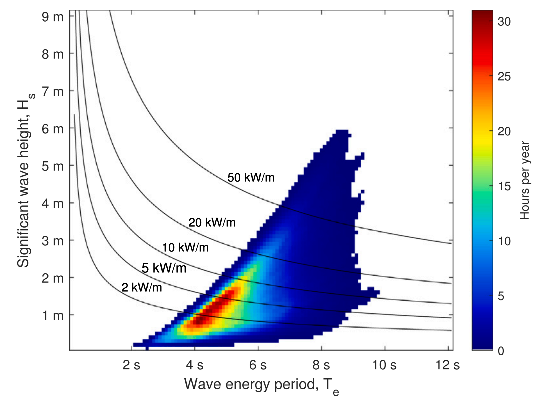

Fig. 8. Wave energy climate 2017–2021.

Table 2
CF and CoV for all the considered cases.

Case	Case 1			Case 2			Case 3			Benchmark		
Subcase	A	B	C	A	B	C	A	B	C	A	B	C
CF	0.29	0.32	0.35	0.47	0.48	0.48	0.29	0.32	0.35	0.49	0.49	0.49
CoV	0.66	0.66	0.68	0.79	0.80	0.80	0.65	0.65	0.67	0.81	0.81	0.81

3.2. Modeled power profiles

The energy generation of RESs can be described using the capacity factor (CF), which is equal to the fraction of full load hours. The annual CF of the stand-alone wind power farms is found to be 0.49, which is slightly higher than what is normally reported since neither wake losses nor downtime for maintenance or service are accounted for [45]. The CFs of all the studied cases can be found in Table 2. The average normalized power production for one year, for the cases with a wind power capacity of 700 MW (subcases B), can be seen in Fig. 9.

Even though the CF of all of the considered co-location cases are lower than the benchmark wind power farms, benefits are seen in the variability of the hourly power profile because of power smoothening. Expressed in coefficient of variation (CoV), which is the standard deviation divided by the mean value, the variability is 0.65–0.68 for the HPPs in case 1 and case 3, and 0.79–0.80 for the HPP in case 2, whereas the CoV of the stand-alone wind power farms is 0.81. All the CoVs can be found in Table 2. As wind power and PV power are negatively correlated in the north European climate, the aggregated variability is decreased, as seen in the reduced CoV [46]. Since the available wave energy is highly dependent on wind-generated waves, especially in short fetch seas such as the North Sea, the smoothening is not at all as substantial for the HPP in case 2.

3.3. Capacity credit

The resulting capacity credits of cases 1–3 with varying wind power capacities are shown in Fig. 10. The capacity credits have been averaged for the whole Dutch EEZ. The capacity credits of the benchmark wind power farms are similar to what has previously been reported for wind power [26]. However, as simplifications are made in the process

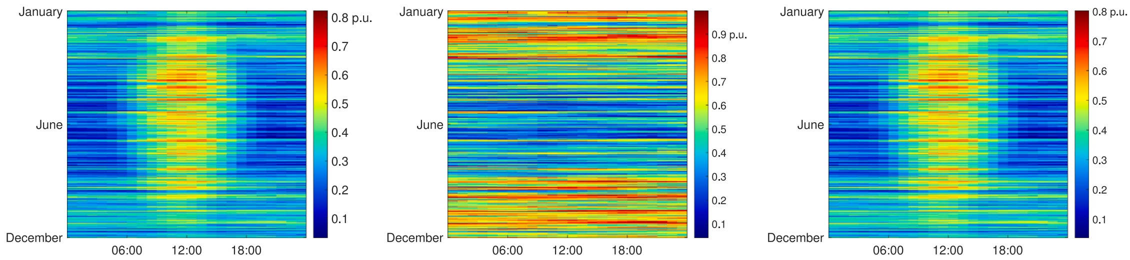

(a) Case 1B (b) Case 2B (c) Case 3B

Fig. 9. Normalized average annual generation for a location far from shore in the Dutch EEZ.

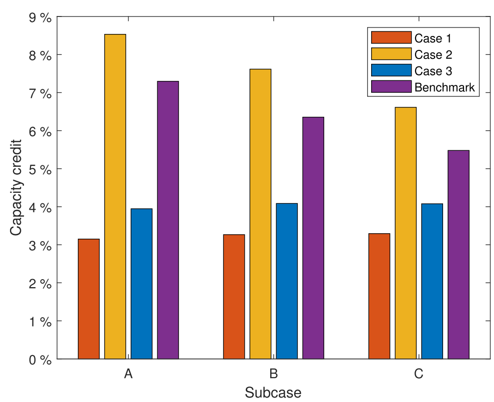

Fig. 10. Capacity credit of the modeled cases.

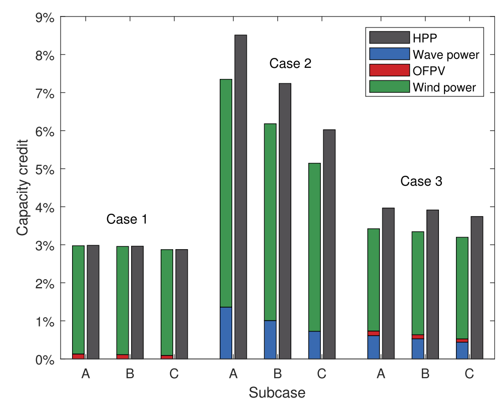

Fig. 11. Capacity credit of the modeled cases compared to non-hybridized installations.

of estimating the capacity credit, less care should be taken for the absolute values, and emphasis is on the relative relationships between the different cases.

As the diurnal and seasonal distribution of PV generation is almost adverse to the load profile of the Netherlands and most higher latitude countries, with typical high load scenarios in the winter months and the morning and afternoon, the added generation from OFPV in case 1 and case 3 decreases the capacity credit of the HPP compared to the benchmark wind power farms. The capacity credit of PV is also lower due to the lower energy yield compared to wind power. The inclusion of wave power in case 2, however, increases the capacity credit compared to the benchmark wind power farm. Both wind power and wave power have an intra-annual cycle with higher energy generation during the winter when the load demand generally is highest.

In Fig. 11, a comparison of the capacity credits of the HPPs and the aggregated capacity credit contributions from the RESs that form the HPPs is shown. The capacity credit of all HPPs is greater than the sum of the respective capacity credit contributions. In other words, the power system reliability contribution is greater for a HPP consisting of 700 MW wind power and 70 MW wave power, than the aggregated power system reliability contribution of 700 MW wind power and 70 MW wave power separately. This is most likely due to the decrease of zero power output hours for the combined power profile, which increases the constant load that can be added to the system.

3.3.1. *Energy storage considerations*

The resulting capacity credits with the addition of BESS with capacities 50 MWh, 150 MWh, and 300 MWh with a maximum discharge and charging rate of 0.25C are found in Table 3. With the EMS aimed at increasing the capacity credit as described in Eq. (6), all studied cases effectively increase the possible added load with the respective maximum power output determined by the C-rate. For example, the addition of a 150 MWh BESS facilitates an added load of 37.5 MW. The BESS capacity is not added to the HPPs nameplate capacity.

3.4. *Retrofitting wind power farms*

A concept that is gaining interest is installing additional generation capacity in existing wind power farms to generate higher revenues without needing additional grid connection points. It is therefore investigated how the co-located energy sources in cases 1–3 would perform if retrofitted to an existing wind power farm with a grid connection capacity equal to the wind farm nameplate capacity. In Fig. 12, the duration curves for all cases are plotted with the grid connection capacity limits marked with dashed lines. Any excess production would need to be curtailed or stored in an energy storage co-located with the plant to avoid violating the grid connection agreement.

Table 4 summarizes the annual added energy generation from the co-located energy sources and the amount that would need to be curtailed for each respective case, with the consideration of BESSs with capacities 50 MWh, 150 MWh, and 300 MWh. The EMS employed in this section is the one intended to reduce curtailment losses, as described in Eq. (7). As expected, the marginal benefit is decreasing with BESS capacity. In other words, the BESS with 150 MWh capacity does not triple the reduced curtailment as compared to the BESS with 50 MWh capacity.

Even though the excess energy generation is substantially smaller in case 2 compared to cases 1 and 3, a higher fraction of the generation needs to be curtailed. The addition of a BESS has a smaller benefit for case 2, as wave power and wind power generally are positively correlated [47], and long consecutive periods of high generation occur leading to a fully charged BESS. For cases 1 and 3, the addition of a BESS is marginally more effective since the generation profile of OFPV follows a diurnal pattern, so no longer consecutive periods of high power output exist. However, it is evident that co-locating negatively correlated sources such as OFPV and wind power, is more effective than using a BESS to increase the utilization of an existing grid connection point. If retrofitting OFPV or wave power into an existing offshore wind power farm, lower capacities than what is considered in these

Table 3
Capacity credit of all cases with additional energy storage.

	Subcase	Capacity credit, with BESS capacity			
		0 MWh	50 MWh	150 MWh	300 MWh
Case 1	A	2.98%	4.19%	6.28%	9.40%
	B	2.96%	4.16%	5.94%	8.62%
	C	2.88%	4.03%	5.50%	7.71%
Case 2	A	8.51%	10.70%	15.10%	21.70%
	B	7.24%	9.24%	12.50%	17.30%
	C	6.02%	7.78%	10.10%	13.60%
Case 3	A	3.97%	4.93%	6.90%	9.85%
	B	3.91%	4.93%	6.63%	9.19%
	C	3.74%	4.78%	6.20%	8.31%
Benchmark	A	6.83%	9.80%	14.80%	22.30%
	B	5.69%	8.14%	11.70%	17.10%
	C	4.73%	6.73%	9.23%	13.00%

Table 4
Additional energy generation from co-located sources and curtailment of the additional generation.

	Energy generation from co-located sources [GWh]	Subcase	Curtailed generation from co-located sources, with BESS capacity			
			0 MWh	50 MWh	150 MWh	300 MWh
Case 1	893	A	31.3%	30.4%	28.7%	26.4%
		B	25.1%	24.4%	23.2%	21.6%
		C	22.1%	21.6%	20.5%	19.1%
Case 2	165	A	61.6%	58.5%	53.5%	47.8%
		B	61.3%	58.1%	53.1%	47.3%
		C	61.1%	57.9%	52.8%	47.0%
Case 3	1058	A	36.5%	35.7%	34.2%	32.1%
		B	30.9%	30.3%	29.1%	27.6%
		C	28.2%	27.7%	26.7%	25.3%

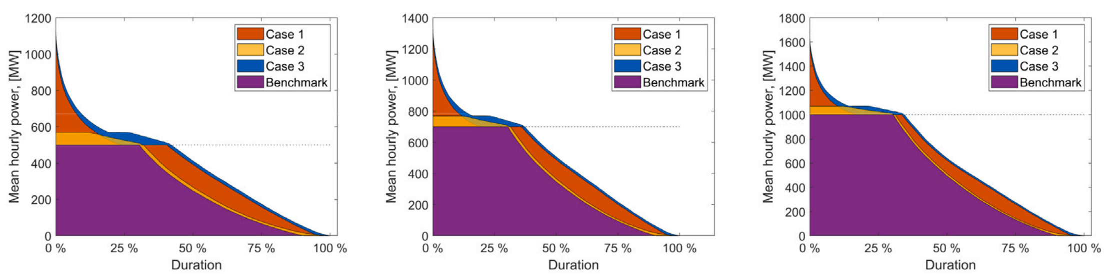

(a) Subcases A (b) Subcases B (c) Subcases C

Fig. 12. Retrofitting an existing wind power farm with a power rating of (a) 500 MW, (b) 700 MW, and (c) 1000 MW. The dashed line marks the grid connection capacity.

cases could be more viable, considering the relatively large fraction of curtailed energy in Table 4.

3.5. Conditional relative frequency distributions

To further investigate the dynamics behind the differentiated grid impact of the three cases, the conditional relative frequency distributions are assessed between OFPV, wave, and wind power. In Fig. 13, the conditional relative frequency distribution of OFPV-wind power, OFPV-wave power, and wave-wind power are shown. The figures represent the occurrence frequency of a value in the y-axis given the corresponding value in the x-axis, such as the conditional probability $P(y \mid x)$. The bin size of the distributions is 0.01 p.u.

As can be seen in Fig. 13(c), high power output states from wind and wave power have a high probability of coinciding, which is natural since wind generates waves. Even though, as can be seen in Fig. 10, the capacity credit of a wave-wind plant, such as in case 2, is higher than that of all other cases. The reason for this is that the electrical load of the Netherlands is highest during the winter months, which is when both wind and wave power produce at their maximum during the intra-annual time scale. The energy generation during the winter months is somewhat smoothed though, why the capacity credit is higher than the benchmark wind power farm. As can be seen in both Figs. 13(a) and 13(b), the probability of high power OFPV output is higher at low wind and wave power output. This decreases the risk of a standstill with zero power output, especially at low wind speeds and low energy sea state situations, which increases the energy availability.

4. Discussion

In this study, three different cases of co-located offshore VRESs have been analyzed and compared to benchmark stand-alone wind power farms. It is found that co-locating wave power with offshore wind power, as in case 2, yields the highest capacity credit for the studied region. Both wave power and wind power generate higher amounts of energy during winter months than summer months, which correlates well with general high loads in countries with similar climates as the Netherlands. This in effect will result in a higher capacity credit than for OFPV, which have the opposite seasonal cycle. Additionally, the CF of OFPV is smaller than both wave and wind, which also leads to a smaller capacity credit for OFPV. It is therefore not unexpected that the capacity credits for case 1 are smaller than those for case 3, and

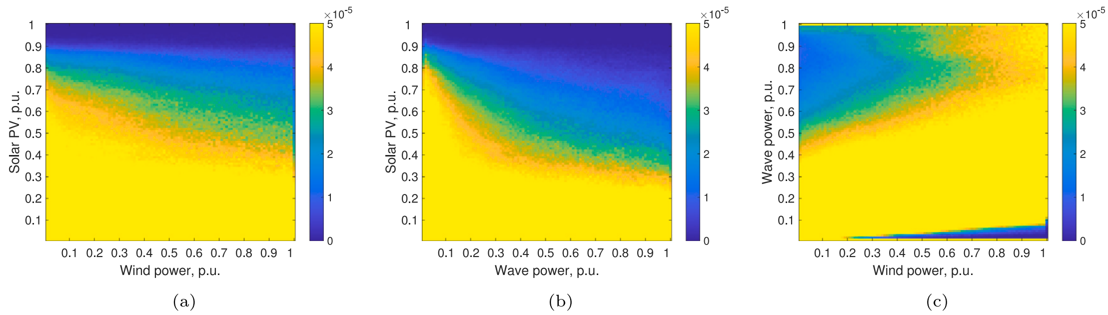

Fig. 13. Conditional relative frequency distributions of (a) OFPV power with regards to wind power, (b) OFPV power with regards to wave power and (c) wave power with regards to wind power.

especially case 2. The added benefit, in terms of capacity credit, of combining wave and wind power appears to be higher than combining wind power and OFPV, when comparing the capacity credit of the HPPs and the aggregated capacity credit contributions from the sources comprising the HPPs. This addresses a shortcoming in assessing complementarity of VRESs using only correlation coefficient, which often is the case, as wind and wave power generally are positively correlated and wind power and OFPV are generally negatively correlated in the North Sea region [47]. The inclusion of a BESS can further increase the capacity credit. In the studied cases, the limiting factor is the maximum discharging power of the BESS.

Even though co-locating OFPV with offshore wind power does not increase the capacity credit, the addition of OFPV to existing wind power farms, as in case 1, shows the greatest possibility of utilizing additional energy generation from the co-located sources, considering a grid connection capacity of the existing wind power farm. In power systems with sufficient operating reserves, retrofitting offshore wind power farms with OFPV facilitates increased energy generation from RESs without additional power grid infrastructure. The addition of a BESS could further decrease the necessary curtailment of the additional generation. With strategic EMS schemes it is likely possible to combine both benefits, as the EMS aimed at increasing the capacity credit leads to an idling BESS most of the time. This would, however, require accurate forecasts of the load and generation to ensure that the BESS has sufficient SoC to discharge at the times when the load exceeds available power generation.

The complementarity of the energy sources is analyzed using conditional relative frequency distribution as compared to the commonly employed correlation coefficient [4]. Even though the correlation coefficient describes the linear relationship, analyzing this phenomenon using conditional relative frequency distribution yields more information on the non-linear relationship between the energy sources. Assessing complementarity using this method in future studies might yield new insights and deepen the knowledge.

4.1. Validity of results

The use of reanalysis meteorological data, as in this study, is commonly employed to model time series of renewable energy generation for various studies on renewable energy integration. Ideally, measurements of installed generation units should be employed. However, as there are no existing energy generation plants corresponding to the analyzed cases under operation, the use of time series modeling is necessary. To the authors' knowledge, no long-term meteorological measurements exist covering all the needed variables, why using reanalysis data in this study is inevitable. ERA5 has been extensively validated in several previous studies, see, for example, Refs. [48–51]. In the application of modeling large-scale wind farms, ERA5 data has been shown to produce accurate energy generation simulations [52]. As for solar radiation, the reanalysis dataset generally overestimates the radiation in cloudy conditions and slightly underestimates the radiation under clear sky conditions [53]. Regarding the estimations of wave parameters, wave height and wave energy period, the reanalysis dataset shows poor agreement with measurement nearshore, since the model employed in ERA5 is based on deep water approximations [54,55]. The dataset has also been shown to underestimate the occurrence of steep waves with wave heights above 8 m and overestimate the occurrence of most common wave heights of 1.75–2 m [51]. In this study, one limitation is the fact that ERA5 reanalysis obtains the wave climate parameters based on deep water approximations, making these results not relevant for nearshore applications [55]. However, as a relatively extensive geographical area is included in the study this likely does not affect the overall results for locations far from the shore. To further analyze the behavior of the HPPs in near-shore locations, specific wave climate models such as the SWAN model [56] could be employed, which is beyond the scope of this study.

4.2. Grid impact on other time scales

Wind, wave, and solar power are characterized by a low degree of predictability and a high degree of variability, that is, the source can change on a time scale from minutes to years [57]. Evidently, it becomes necessary to consider how energy and power are managed, for example, how different energy sources are combined to ensure that power is always available, as in this study. However, for RESs, power quality issues are also of importance, since a power electronic interface with the grid often will be required [58]. A converter-based power generation system can potentially have a significant adverse impact on the electrical grid [59–62]. A first observation is that the use of power electronic converters means that the stabilizing effect on the grid achieved by synchronous generators is lost [59]. Furthermore, renewable energy systems with power converters are usually associated with large harmonic emissions. The emission is inherent in the intermittency of the power production and the nonlinearities of the power converter [63]. The harmonic emissions can be reduced with the use of filters or advanced control schemes [64]. For a practical implementation, it is important to consider how these factors affect the grid and not just the power management at an hourly time scale. It should, however, be observed that many of these issues are highly dependent on the specific choice of technology. For example, the harmonic emission is highly dependent on the specific converter topology and control method [63]. Therefore, it is difficult to give any generalized recommendations. These types of issues are more suitable to study on a detailed case-by-case basis.

5. Conclusions

Of the three cases considered in this study, co-locating wind and wave, as in case 2, yields the highest capacity credit. Co-locating wind and OFPV, as in case 1, yields a significantly lower capacity credit, and co-locating all three sources, as in case 3, results in a capacity credit higher than for case 1, but smaller than case 2. This shows that the benefit for the power system of co-locating RESs that have a seasonal generation profile similar to the seasonal profile of the system load can be higher than for RESs with generation profiles that are negatively correlated, which often is used to assess the complementarity. If there are sufficient operating reserves, however, negatively correlated RESs such as wind power and OFPV is suitable to co-locate to increase the utilization of the grid connection point. By combining a HPP with a BESS of the sizes considered in this study, the possible load added to the system without decreasing the reliability can be increased, equal to the maximum discharge rate of the BESS. Using a BESS to reduce curtailment when co-locating VRESs in existing wind power farms can also reduce the necessary curtailment, but it is more effective to co-locate negatively correlated VRESs.

In all studied scenarios, it is noteworthy that the capacity credit of the entire HPP exceeds the capacity contribution of the individual sources comprising the HPP. In other words, the energy reliability of a HPP consisting of 700 MW wind power and 70 MW wave power is higher than the aggregated reliability of the separate wind power farm and wave power farm. This means that it is vital to address the joint power profile when analyzing the grid impact of an HPP, and in extension, that higher penetration levels of VRESs can be integrated into the system without decreased reliability.

This study also shows that co-locating VRESs can serve different purposes. Adding OFPV to wind power farms should primarily be done with the purpose of delivering larger amounts of energy to the grid, which effectively can be achieved. Combining wind power and wave power is ineffective in achieving the same purpose, but instead provides a higher capacity credit. As the share of VRESs in the power system is increasing, it is important to not only address energy generation but to also consider reliability and availability aspects, such as the ones provided by co-locating wave power and wind power.

CRediT authorship contribution statement

Erik Jonasson: Writing – review & editing, Writing – original draft, Methodology, Formal analysis, Conceptualization. **Christoffer Fjellstedt:** Writing – review & editing, Writing – original draft, Conceptualization. **Irina Temiz:** Writing – review & editing, Supervision, Funding acquisition.

Declaration of competing interest

The authors declare that they have no known competing financial interests or personal relationships that could have appeared to influence the work reported in this paper.

Acknowledgments

This work has received support from STandUP for Energy, Uppsala University and the EU-SCORES project financed by the European Union's Horizon 2020 and Green Deal Research and Innovation Programme under grant agreement No 101036457.

References

[1] International Energy Agency, World Energy Outlook 2023, Tech. Rep., International Energy Agency, 2023.
[2] European Union, An EU strategy to harness the potential of offshore renewable energy for a climate, 2020.
[3] S. Guo, Q. Liu, J. Sun, H. Jin, A review on the utilization of hybrid renewable energy, Renew. Sustain. Energy Rev. 91 (2018) 1121–1147, http://dx.doi.org/10.1016/J.RSER.2018.04.105.
[4] S. Upadhyay, M.P. Sharma, A review on configurations, control and sizing methodologies of hybrid energy systems, Renew. Sustain. Energy Rev. 38 (2014) 47–63, http://dx.doi.org/10.1016/J.RSER.2014.05.057.
[5] H. Hou, T. Xu, X. Wu, H. Wang, A. Tang, Y. Chen, Optimal capacity configuration of the wind-photovoltaic-storage hybrid power system based on gravity energy storage system, Appl. Energy 271 (2020) 115052, http://dx.doi.org/10.1016/J.APENERGY.2020.115052.
[6] A.A. Prasad, Y. Yang, M. Kay, C. Menictas, S. Bremner, Synergy of solar photovoltaics-wind-battery systems in Australia, Renew. Sustain. Energy Rev. 152 (2021) 111693, http://dx.doi.org/10.1016/J.RSER.2021.111693.
[7] C. Pérez-Collazo, D. Greaves, G. Iglesias, A review of combined wave and offshore wind energy, Renew. Sustain. Energy Rev. 42 (2015) 141–153, http://dx.doi.org/10.1016/J.RSER.2014.09.032.
[8] H.D.P. Gonzalez, F.D. Bianchi, J.L. Dominguez-Garcia, O. Gomis-Bellmunt, Co-located wind-wave farms: Optimal control and grid integration, Energy 272 (2023) 127176, http://dx.doi.org/10.1016/J.ENERGY.2023.127176.
[9] S.Z. Golroodbari, D.F. Vaartjes, J.B. Meit, A.P. van Hoeken, M. Eberveld, H. Jonker, W.G. van Sark, Pooling the cable: A techno-economic feasibility study of integrating offshore floating photovoltaic solar technology within an offshore wind park, Sol. Energy 219 (2021) 65–74, http://dx.doi.org/10.1016/J.SOLENER.2020.12.062.
[10] N. Pearre, K. Adye, L. Swan, Proportioning wind, solar, and in-stream tidal electricity generating capacity to co-optimize multiple grid integration metrics, Appl. Energy 242 (2019) 69–77, http://dx.doi.org/10.1016/j.apenergy.2019.03.073.
[11] S. Astariz, G. Iglesias, Enhancing wave energy competitiveness through co-located wind and wave energy farms. A review on the shadow effect, Energies 8 (2015) 7344–7366, http://dx.doi.org/10.3390/EN8077344, 2015, Vol. 8, Pages 7344-7366.
[12] E. Gubesch, N.Y. Sergiienko, J.-R. Nader, B. Ding, B. Cazzolato, I. Penesis, Y. Li, Experimental investigation of a co-located wind and wave energy system in regular waves, Renew. Energy 219 (2023) 119520, http://dx.doi.org/10.1016/J.RENENE.2023.119520.
[13] E.D. Stoutenburg, N. Jenkins, M.Z. Jacobson, Power output variations of co-located offshore wind turbines and wave energy converters in California, Renew. Energy 35 (2010) 2781–2791, http://dx.doi.org/10.1016/J.RENENE.2010.04.033.
[14] S. Rasool, K.M. Muttaqi, D. Sutanto, M. Hemer, Quantifying the reduction in power variability of co-located offshore wind-wave farms, Renew. Energy 185 (2022) 1018–1033, http://dx.doi.org/10.1016/J.RENENE.2021.12.120.
[15] E. Rusu, F. Onea, A parallel evaluation of the wind and wave energy resources along the latin American and European coastal environments, Renew. Energy 143 (2019) 1594–1607, http://dx.doi.org/10.1016/J.RENENE.2019.05.117.
[16] Y. Wen, B. Kamranzad, P. Lin, Joint exploitation potential of offshore wind and wave energy along the south and southeast coasts of China, Energy 249 (2022) 123710, http://dx.doi.org/10.1016/J.ENERGY.2022.123710.
[17] M. López, N. Rodríguez, G. Iglesias, Combined floating offshore wind and solar PV, J. Mar. Sci. Eng. 8 (2020) 576, http://dx.doi.org/10.3390/JMSE8080576, 2020, Vol. 8, Page 576.
[18] F. Fusco, G. Nolan, J.V. Ringwood, Variability reduction through optimal combination of wind/wave resources – An Irish case study, Energy 35 (2010) 314–325, http://dx.doi.org/10.1016/J.ENERGY.2009.09.023.
[19] D.A. Halamay, T.K. Brekken, A. Simmons, S. McArthur, Reserve requirement impacts of large-scale integration of wind, solar, and ocean wave power generation, IEEE Trans. Sustain. Energy 2 (2011) 321–328, http://dx.doi.org/10.1109/TSTE.2011.2114902.
[20] International Energy Agency, World energy statistics and balances, 2023.
[21] C. wei Zheng, Z. niu Xiao, Y. hua Peng, C. yin Li, Z. bo Du, Rezoning global offshore wind energy resources, Renew. Energy 129 (2018) 1–11, http://dx.doi.org/10.1016/J.RENENE.2018.05.090.
[22] A.V. Meier, Integration of renewable generation in California: Coordination challenges in time and space, in: Proceeding of the International Conference on Electrical Power Quality and Utilisation, EPQU, 2011, pp. 768–773, http://dx.doi.org/10.1109/EPQU.2011.6128888.
[23] B. Sandén, Systems perspectives on renewable power, 2014, URL https://research.chalmers.se/publication/210498.
[24] S. Renewables, The benefits of pumped storage hydro to the UK, 2016.
[25] L.L. Garver, Effective load carrying capability of generating units, IEEE Trans. Power Appar. Syst. PAS-85 (1966) 910–919, http://dx.doi.org/10.1109/TPAS.1966.291652.
[26] C. Ensslin, M. Milligan, H. Holttinen, M. O'Malley, A. Keane, Current methods to calculate capacity credit of wind power, in: Proc. IEEE Power Energy Soc. General Meeting, 2008, pp. 1–3, http://dx.doi.org/10.1109/PES.2008.4596006.
[27] C. Dent, A. Keane, J. Bialek, Simplified methods for renewable generation capacity credit calculation: A critical review, in: Proc. IEEE Power Energy Soc. General Meeting, 2010, pp. 1–8, http://dx.doi.org/10.1109/PES.2010.5589606.
[28] L. Soder, M. Amelin, A review of different methodologies used for calculation of wind power capacity credit, in: Proc. IEEE Power Energy Soc. General Meeting, 2008, pp. 1–5, http://dx.doi.org/10.1109/PES.2008.4596666.
[29] C.D.S. Copernicus Climate Change Service, ERA5 hourly data on single levels from 1940 to present, 2023, http://dx.doi.org/10.24381/cds.adbb2d47.
[30] ENTSO-E, Transparency platform, 2023, URL https://transparency.entsoe.eu/. (Accessed 17 October 2023).
[31] The ENTSO-E transparency platform – A review of Europe's most ambitious electricity data platform, Appl. Energy 225 (2018) 1054–1067, http://dx.doi.org/10.1016/J.APENERGY.2018.04.048.

[32] CorPower Ocean, 2023, URL https://corpowerocean.com/. (Accessed 16 October 2023).
[33] A. Babarit, On the park effect in arrays of oscillating wave energy converters, Renew. Energy 58 (2013) 68–78, http://dx.doi.org/10.1016/J.RENENE.2013.03.008.
[34] R. Satymov, D. Bogdanov, M. Dadashi, G. Lavidas, C. Breyer, Techno-economic assessment of global and regional wave energy resource potentials and profiles in hourly resolution, Appl. Energy 364 (2024) 123119, http://dx.doi.org/10.1016/J.APENERGY.2024.123119.
[35] R. Claus, M. López, Key issues in the design of floating photovoltaic structures for the marine environment, Renew. Sustain. Energy Rev. 164 (2022) 112502, http://dx.doi.org/10.1016/J.RSER.2022.112502.
[36] S. Dubey, J.N. Sarvaiya, B. Seshadri, Temperature dependent photovoltaic (PV) efficiency and its effect on PV production in the world – A review, Energy Procedia 33 (2013) 311–321, http://dx.doi.org/10.1016/J.EGYPRO.2013.05.072.
[37] W. Musial, P. Beiter, S. Tegen, A. Smith, Potential Offshore Wind Energy Areas in Californa: An Assessment of Locations, Technology and Costs, Tech. Rep., National Renewable Energy Laboratory, 2016.
[38] S.A. Hsu, E.A. Meindl, D.B. Gilhousen, Determining the power-law wind-profile exponent under near-neutral stability conditions at sea, J. Appl. Meteorol. (1988-2005) 33 (6) (1994) 757–765.
[39] P. Nørgaard, H. Holttinen, A multi-turbine power curve approach, 2004.
[40] J. Olauson, M. Bergkvist, Modelling the Swedish wind power production using MERRA reanalysis data, Renew. Energy 76 (2015) 717–725, http://dx.doi.org/10.1016/J.RENENE.2014.11.085.
[41] E.C. Malz, V. Walter, L. Göransson, S. Gros, The value of airborne wind energy to the electricity system, Wind Energy 25 (2022) 281–299, http://dx.doi.org/10.1002/WE.2671.
[42] EU-SCORES, 2023, URL https://euscores.eu/. (Accessed 16 October 2023).
[43] R.A. Campos, L.R. do Nascimento, R. Rüther, The complementary nature between wind and photovoltaic generation in Brazil and the role of energy storage in utility-scale hybrid power plants, Energy Convers. Manage. 221 (2020) 113160, http://dx.doi.org/10.1016/J.ENCONMAN.2020.113160.
[44] Dutch Offshore Wind Atlas, 2024, URL https://www.dutchoffshorewindatlas.nl/. (Accessed 23 April 2024).
[45] N. Boccard, Capacity factor of wind power realized values vs. estimates, Energy Policy 37 (2009) 2679–2688, http://dx.doi.org/10.1016/J.ENPOL.2009.02.046.
[46] J. Widén, Correlations between large-scale solar and wind power in a future scenario for Sweden, IEEE Trans. Sustain. Energy 2 (2011) 177–184, http://dx.doi.org/10.1109/TSTE.2010.2101620.
[47] E. Jonasson, I. Temiz, Grid value of co-located offshore renewable energy, in: Proceedings of the European Wave and Tidal Energy Conference, Vol. 15, 2023, http://dx.doi.org/10.36688/ewtec-2023-313.
[48] W. Tang, J. Qin, K. Yang, F. Zhu, X. Zhou, Does ERA5 outperform satellite products in estimating atmospheric downward longwave radiation at the surface? Atmos. Res. 252 (2021) 105453, http://dx.doi.org/10.1016/J.ATMOSRES.2021.105453.
[49] D. Tetzner, E. Thomas, C. Allen, A validation of ERA5 reanalysis data in the southern Antarctic peninsula — Ellsworth land region, and its implications for ice core studies, Geosciences 9 (2019) 289, http://dx.doi.org/10.3390/GEOSCIENCES9070289, 2019, Vol. 9, Page 289.
[50] K. Gruber, P. Regner, S. Wehrle, M. Zeyringer, J. Schmidt, Towards global validation of wind power simulations: A multi-country assessment of wind power simulation from MERRA-2 and ERA-5 reanalyses bias-corrected with the global wind atlas, Energy 238 (2022) 121520, http://dx.doi.org/10.1016/J.ENERGY.2021.121520.
[51] M. Alday, V. Raghavan, G. Lavidas, Analysis of the North Atlantic offshore energy flux from different reanalysis and hindcasts, in: Vol. 15: (2023): Proceedings of the European Wave and Tidal Energy Conference, 2023.
[52] J.P. Murcia, M.J. Koivisto, G. Luzia, B.T. Olsen, A.N. Hahmann, P.E. Sørensen, M. Als, Validation of European-scale simulated wind speed and wind generation time series, Appl. Energy 305 (2022) 117794, http://dx.doi.org/10.1016/J.APENERGY.2021.117794.
[53] R. Urraca, T. Huld, A. Gracia-Amillo, F.J.M. de Pison, F. Kaspar, A. Sanz-Garcia, Evaluation of global horizontal irradiance estimates from ERA5 and COSMO-REA6 reanalyses using ground and satellite-based data, Sol. Energy 164 (2018) 339–354, http://dx.doi.org/10.1016/J.SOLENER.2018.02.059.
[54] H. Shi, X. Cao, Q. Li, D. Li, J. Sun, Z. You, Q. Sun, Evaluating the accuracy of ERA5 wave reanalysis in the water around China, J. Ocean Univ. China 20 (2021) 1–9, http://dx.doi.org/10.1007/S11802-021-4496-7/METRICS.
[55] F. Barbariol, S. Davison, F.M. Falcieri, R. Ferretti, A. Ricchi, M. Sclavo, A. Benetazzo, Wind waves in the Mediterranean sea: An ERA5 reanalysis wind-based climatology, Front. Mar. Sci. 8 (2021) 760614, http://dx.doi.org/10.3389/FMARS.2021.760614/BIBTEX.
[56] Delft University of Technology, SWAN - Simulating Waves Nearshore. URL https://swanmodel.sourceforge.io/.
[57] O. Edenhofer, R.P. Madruga, Y. Sokona, K. Seyboth, P. Matschoss, S. Kadner, T. Zwickel, P. Eickemeier, G. Hansen, S. Schlömer, C. von Stechow, Renewable energy sources and climate change mitigation - Special report of the intergovernmental panel on climate change, 2016.
[58] F. Blaabjerg, K. Ma, Wind energy systems, Proc. IEEE 105 (2017) 2116–2131, http://dx.doi.org/10.1109/JPROC.2017.2695485.
[59] J. Shair, H. Li, J. Hu, X. Xie, Power system stability issues, classifications and research prospects in the context of high-penetration of renewables and power electronics, Renew. Sustain. Energy Rev. 145 (2021) 111111, http://dx.doi.org/10.1016/J.RSER.2021.111111.
[60] B.M.S. Hodge, H. Jain, C. Brancucci, G.S. Seo, M. Korpås, J. Kiviluoma, H. Holttinen, J.C. Smith, A. Orths, A. Estanqueiro, L. Söder, D. Flynn, T.K. Vrana, R.W. Kenyon, B. Kroposki, Addressing technical challenges in 100% variable inverter-based renewable energy power systems, Wiley Interdiscip. Rev.: Energy Environ. 9 (2020) e376, http://dx.doi.org/10.1002/WENE.376.
[61] B. Shakerighadi, N. Johansson, R. Eriksson, P. Mitra, A. Bolzoni, A. Clark, H.P. Nee, An overview of stability challenges for power-electronic-dominated power systems: The grid-forming approach, IET Gener. Transm. Distrib. 17 (2023) 284–306, http://dx.doi.org/10.1049/GTD2.12430.
[62] S.T. Meraj, S.S. Yu, M.S. Rahman, K. Hasan, M.S.H. Lipu, H. Trinh, Energy management schemes, challenges and impacts of emerging inverter technology for renewable energy integration towards grid decarbonization, J. Clean. Prod. 405 (2023) 137002, http://dx.doi.org/10.1016/J.JCLEPRO.2023.137002.
[63] F. Blaabjerg, Y. Yang, K.A. Kim, J. Rodriguez, Power electronics technology for large-scale renewable energy generation, Proc. IEEE 111 (2023) 335–355, http://dx.doi.org/10.1109/JPROC.2023.3253165.
[64] X. Liang, C. Andalib Bin-Karim, Harmonics and mitigation techniques through advanced control in grid-connected renewable energy sources: A review, IEEE Trans. Ind. Appl. 54 (4) (2018) 3100–3111, http://dx.doi.org/10.1109/TIA.2018.2823680.